

Calculation of Electronic and Optical Properties of Doped Titanium Dioxide Nanostructure

Shokoufeh Khaleghi *

Department of Micro- and Nanoelectronics, Belarusian State University of Informatics and Radioelectronics
P. Browka 6, 220013, Minsk, Belarus

Article history:

Received 3/6/2012

Accepted 11/8/2012

Published online 1/9/2012

Keywords:

TiO₂, Band-gap engineering,

Absorption coefficient,

Nanostructures.

**Corresponding author:*

E-mail address:

khaleghi.shokoufeh@gmail.com

Phone: +375292729252

Fax: +375172021033

Abstract

By means of first principles calculations we show that both rutile and anatase phases of bulk TiO₂ doped by S, Se or Pb can display substantial decreasing in the band gap (up to 50%), while doping by Zr does not sizably affect the band-gap value. Moreover, the absorption edge is shifted (up to 1 eV) to the lower energy range in the case of TiO₂ doped by S or Pb that opens a way to enhancing of absorption of sun's radiation. We also discuss how our findings can improve efficiency of photovoltaic cells and photocatalytic cells for hydrogen generation.

2012 JNS All rights reserved

1. Introduction

Titanium dioxide (TiO₂) displaying perfect chemical stability and oxidative ability can be considered as the most investigated material among metal oxides because it is used in a wide range of applications [1,2] including photocatalysis and photovoltaics. TiO₂ is characterized by the band gap of 3.0 eV (the rutile phase) and 3.2 eV (the anatase phase) indicating that only a small fraction of the sun's energy (mainly ultraviolet region) will be utilized in solar energy conversion and water splitting processes. To absorb visible light TiO₂ is usually doped or sensitized [2].

Doping both by metal and nonmetal atoms can be easily achieved during anodization procedure which is a rather facile method prepare TiO₂.

In this paper we performed first principles calculations in order to reveal changes in a band structure and in the absorption coefficient of the bulk TiO₂ with the rutile and anatase phases doped by Zr, Pb, S or Se. Our main goal is to find a doping material which can efficiently reduce the band gap by 1 – 1.3 eV and, at the same time, provide a shift in the absorption edge to the lower energy range.

2. Computational details and structural models

The anatase phase of TiO_2 has the tetragonal structure (the space group $I41/amdS$) and the following lattice parameters: $a = 3.7842 \text{ \AA}$, $c = 9.5146 \text{ \AA}$ [1]. In the unit cell there are four Ti atoms and eight O atoms which are grouped in one chemically inequivalent type both for Ti and O atoms. The rutile phase of TiO_2 is also characterized by the tetragonal structure (the space group $P42/mnm$) with $a = 4.5922 \text{ \AA}$, $c = 2.9590 \text{ \AA}$ [1]. The unit cell consists of two Ti atoms and four O atoms.

The full structural optimizations as well as the total energy calculations of bulk TiO_2 were performed within density-functional theory using the Vienna ab initio simulation package (code VASP) [3-5] with a plane-wave basis set. The generalized gradient approximation of Perdew–Burke–Ernzerhof [6] was utilized in the calculations. Total energy minimization was obtained by calculating of Hellmann-Feynman forces and the stress tensor. The atomic relaxation was stopped when forces on atoms were less than 0.01 eV/\AA . The energy cutoff of 300 eV was applied, while the $13 \times 13 \times 7$ and $9 \times 9 \times 15$ meshes of Monkhorst-Pack points were used for the anatase and rutile phases, respectively. The self-consistent procedure was continued until the difference between the total energies in two successive iterations was less than 1 meV/atom .

In order to model doped bulk TiO_2 we have increased the unit cell. In this case it is possible to reduce the doping concentration. Thus, the supercells $2 \times 2 \times 1$ for the anatase phase and $2 \times 2 \times 2$ for the rutile phase were formed, which are shown in Figures 1 and 2, respectively. The self-consistent procedure were carried out on $5 \times 5 \times 8$ and $7 \times 7 \times 5$ \mathbf{k} -

point meshes. The band structure calculations have been performed on the self-consistent charge density.

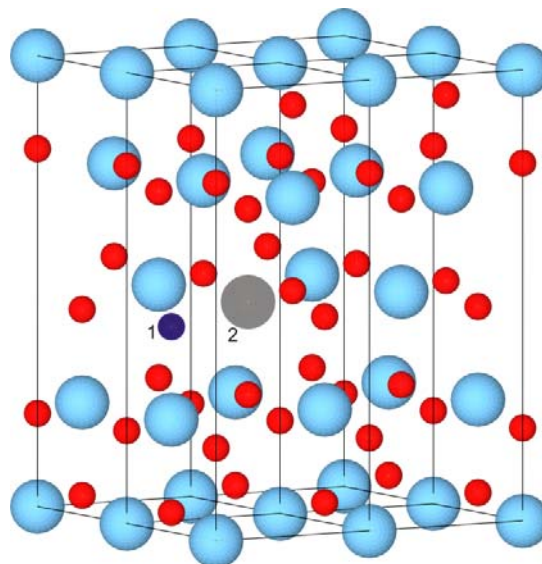


Fig. 1. The $2 \times 2 \times 1$ supercell of TiO_2 in the anatase phase which consists of 4 unit cells. The larger balls indicate Ti atoms while smaller balls stand for O atoms. The Ti and O atoms, which are substituted for an impurity atom, are indicated by 1 and 2, respectively.

The optical absorption coefficient has been calculated by using the full-potential linearized augmented plane wave method (WIEN2k package) [7] with the same generalized gradient approximation of Perdew–Burke–Ernzerhof [6]. The fully optimized structural parameters of TiO_2 supercells with different phases have been taken into account. The energy cutoff constant RMTKmax equal to 7 and 60 \mathbf{k} -points uniformly distributed in the irreducible part of the Brillouin zone were found to be sufficient for a self-consistent procedure. The dipole matrix element, which is the key ingredient for optical property calculations, has been evaluated at a dense grid of about 264 \mathbf{k} -points in the irreducible part of the Brillouin zone.

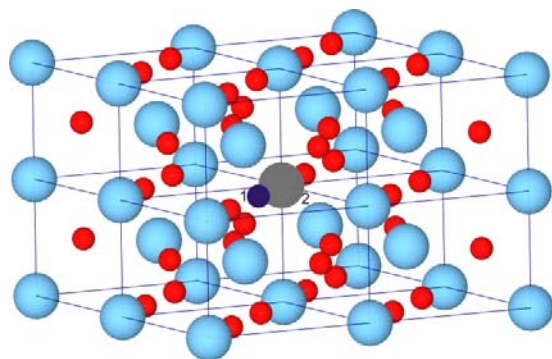


Fig. 2. The $2 \times 2 \times 2$ supercell of TiO_2 in the rutile phase which consists of 8 unit cells. The larger balls indicate Ti atoms while smaller balls stand for O atoms. The Ti and O atoms, which are substituted for an impurity atom, are indicated by 1 and 2, respectively.

3. Results and discussion

After full structural optimization the lattice parameters for bulk TiO_2 are found to be $a = 3.795 \text{ \AA}$, $c = 9.730 \text{ \AA}$ for the anatase phase and $a = 4.584 \text{ \AA}$, $c = 2.953 \text{ \AA}$ for the rutile phase. The results obtained are in good agreement with known experimental data [1].

We have deliberately chosen S and Se atoms to replace an O atom in the supercell since they are in the same VI column in the Periodic Table. Analogous issue is valid for Zr and Pb atoms, which substitute for Ti, because they belong to the IV column. In this case we do not expect metallic or degenerate semiconducting properties to appear in doped TiO_2 due to the same number of the valence electrons.

For the sake of comparison we present the band diagram for pure TiO_2 for the supercell case as for doped TiO_2 . The corresponding band diagrams are shown in Figures 3 and 4 for the anatase and rutile phases, respectively. It is evident that the band gap is reduced in anatase TiO_2 when doped by S (by 34%) or Se (by 46%), while Zr and Pb

incorporation does not affect the gap value (Fig. 3). In the case of the rutile phase the band gap shrinkage is clearly seen for S (by 24%), Se (41%) and Pb (by 27%) doping.

Surprisingly, the absorption coefficient of TiO_2 doped by Se does not show any significant shift to the lower energy range near the absorption edge (Figure 5). In fact it almost coincides with the one for the pure TiO_2 both for the anatase and rutile phases, while TiO_2 doped by S or Pb does display the shift (up to 1 eV) of the absorption coefficient to the lower energy range near the absorption edge.

4. Conclusion

Our first principles results clearly show that TiO_2 doped by S and Pb display both the band-gap reduction and the shift of the absorption coefficient to the lower energy range near the absorption edge with respect to pure TiO_2 independently of the phase. We predict this shift to be about 1 eV indicating that a part of the visible region from sun's irradiation can be now absorbed by such doped TiO_2 . Another factor, which also affects performance of photovoltaic and photocatalytic cells, is charge separation.

Electrons and holes generated under the sun's irradiation should be efficiently separated to avoid their recombination indicating that a material should have good transport properties. Nevertheless, our band structures of TiO_2 doped by S display the top valence band to move upward pointing out formation of an impurity band which can compromise transport properties of this material. Finally, we suggest our findings to be carefully considered in manufacturing of photovoltaic and photocatalytic cells.

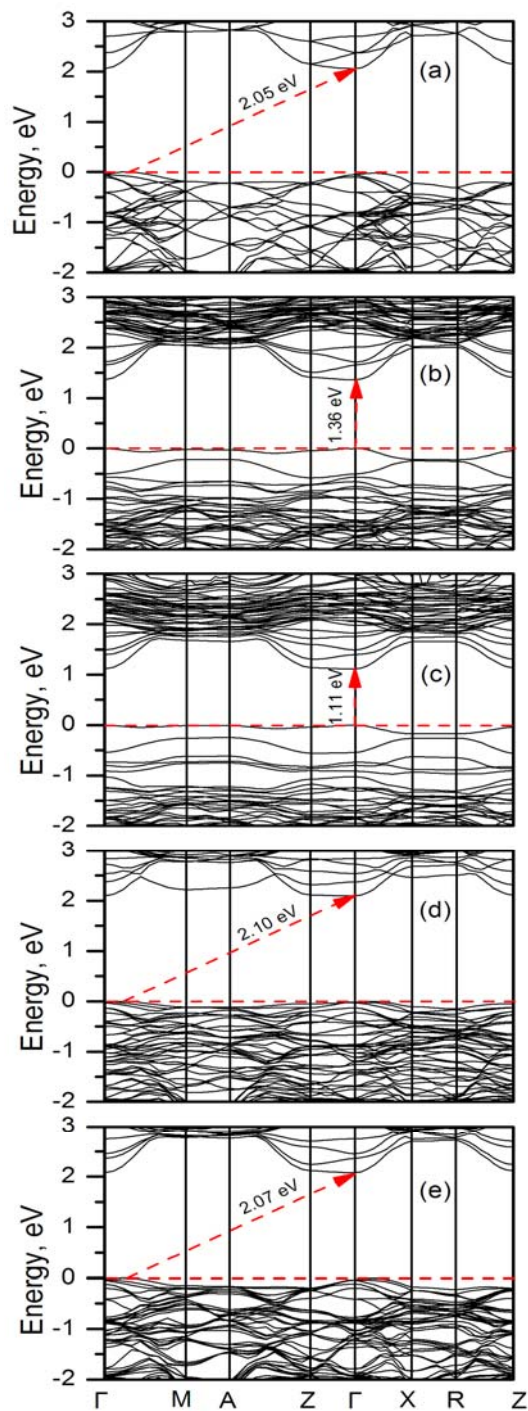


Fig. 3. The band diagrams of pure and doped anatase TiO_2 as calculated along the high symmetry directions of the tetragonal Brillouine zone. Zero at the energy scale corresponds to the top of the valence band. The band-gap values are indicated. (a) pure TiO_2 ; (b) $\text{Ti}_{16}\text{O}_{31}\text{S}$; (c) $\text{Ti}_{16}\text{O}_{31}\text{Se}$; (d) $\text{Ti}_{15}\text{PbO}_{32}$; (e) $\text{Ti}_{15}\text{ZrO}_{32}$.

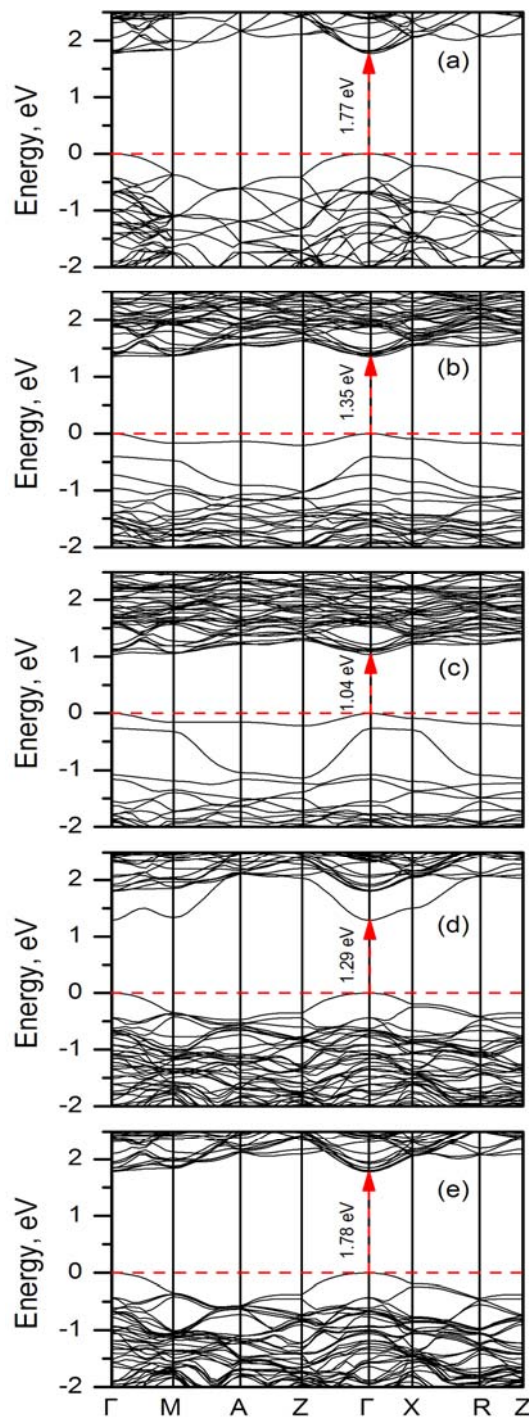


Fig. 4. The band diagrams of pure and doped rutile TiO_2 as calculated along the high symmetry directions of the tetragonal Brillouine zone. Zero at the energy scale corresponds to the top of the valence band. The band-gap values are indicated. (a) pure TiO_2 ; (b) $\text{Ti}_{16}\text{O}_{31}\text{S}$; (c) $\text{Ti}_{16}\text{O}_{31}\text{Se}$; (d) $\text{Ti}_{15}\text{PbO}_{32}$; (e) $\text{Ti}_{15}\text{ZrO}_{32}$.

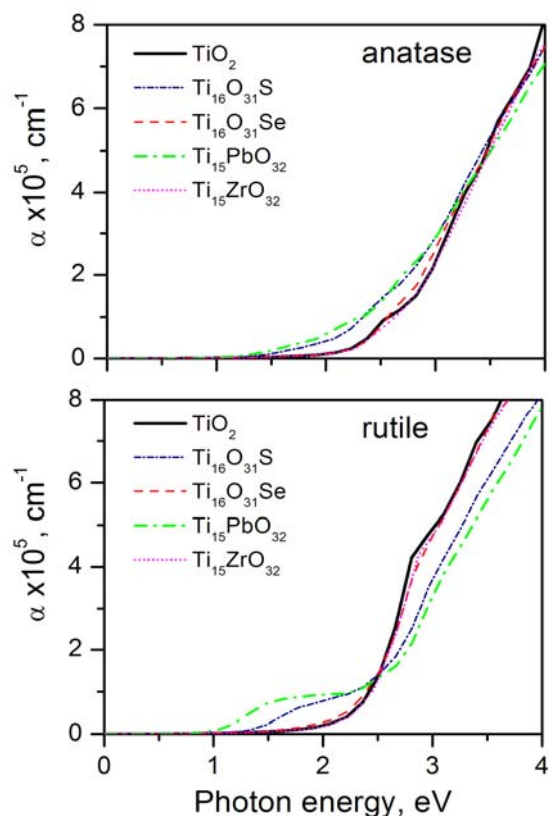


Fig. 5. The absorption coefficient of pure and doped TiO_2 . The phases are indicated.

Acknowledgment

The author is grateful to the Professor V. E. Borisenko and Doctors D.B. Migas, V.L. Shaposhnikov and A.V. Krivosheeva for stimulating discussion on the presented results.

References

- [1] U. Diebold, Surf. Sci. Rep. 48 (2003) 53.
- [2] X. Chen, S. S. Mao, Chem. Rev. 107 (2007) 2891.
- [3] G. Kresse, J. Hafner, Phys. Rev. B. 49 (1994) 14251.
- [4] G. Kresse, J. Furthmüller, Phys. Rev. B. 54 (1996) 11169.
- [5] G. Kresse, J. Furthmüller, Comput. Mater. Sci. 6 (1996) 15.
- [6] J. P. Perdew, K. Burke, M. Ernzerhof, Phys. Rev. Lett. 77 (1996) 3865.
- [7] P. Blaha, K. Schwarz, G. K. H. Madsen, D. Kvasnicka, J. Luitz, WIEN2k, An Augmented Plane Wave + Local Orbitals Program for Calculating Crystal Properties; Karlheinz Schwarz, Techn. Universitat Wien: Austria, 2001. ISBN 3-9501031-1-2.